SPATIAL SPECTRA OF THE EIGENMODES OF RIBBED PLATES PROJECTED ON DISPERSION BRANCHES

G. Lefebvre[1] , X. Boutillon[1*] and M. Filoche[2]

[1]Laboratoire de Mécanique des solides
École polytechnique, 91128 Palaiseau Cedex, FRANCE
Email: lefebvre@lms.polytechnique.fr, boutillon@lms.polytechnique.fr

[2]Laboratoire de Physique de la matière condensée
École polytechnique, 91128 Palaiseau Cedex, FRANCE
Email: marcel.filoche@polytechnique.edu

ABSTRACT

A vast literature has been devoted to the transverse vibration and the sound radiation of ribbed plates over the last decades. The present study has been motivated by the analysis of the dynamical behaviour of piano soundboards. As a rough approximation, a piano soundboard can be considered as an orthotropic ribbed plate. Our purpose is to establish condensed descriptions for their dynamics. For low frequencies, regularly ribbed plates can be considered as homogeneous plates. It is usually considered that homogenization is valid only up to a frequency corresponding roughly to the confinement of one half wave-length between the (periodically spaced) ribs. Beyond that frequency, depending on the relative characteristic mobility of the ribs and that of the base plate, the ribs may constrain transverse waves to be guided between them. We focus here on the spatial spectrum of the normal modes of the ribbed plate (2D Fourier transforms of the modal shapes). It appears that most of the peaks of each spectrum can be seen as belonging to one of a few dispersion branches in an appropriate (ω, k)-plane. Interestingly, different peaks of a spectrum (of one given mode) usually "belong" to different dispersion branches. When valid, this description may prove an interesting intermediate step to derive approximations for the sound radiation of such plates.

1 INTRODUCTION

This study has been motivated by the analysis of the dynamics of piano soundboards, which are sophisticated ribbed plates[1]. We consider here a more simple system which consists in a thin rectangular plate represented in Fig. 1 (axes of the Oxy-frame of reference parallel to the sides of the rectangle, $L_x = 1.39\,\mathrm{m}$, $L_y = 0.91\,\mathrm{m}$, $h = 0.008\,\mathrm{m}$). The regularly-spaced ribs are oriented in the OX-direction ($\theta = (Ox, OX)$ =1.0065 rad), with inter-rib spacing d =0.13 m. Materials are orthotropic (ρ =392 kg m^{-3}, E_X =11.5 × 10^9 Pa, E_Y =0.47 × 10^9 Pa for the main plate and for the ribs, corresponding to one quality of spruce). Note that the geometry does not correspond to the so-called *special orthotropy* configuration ($OX = Ox$) and that (incidentally, not necessarily) the ribs are in the direction of one orthotropy axis. Here, boundary conditions have been chosen as clamped all around the plate.

The plate has been modelled as a thin plate (Kirchhoff-Love theory) and treated by means of FreeFem++, a Finite-element software, yielding the normal modes.

2 MODAL SPECTRA

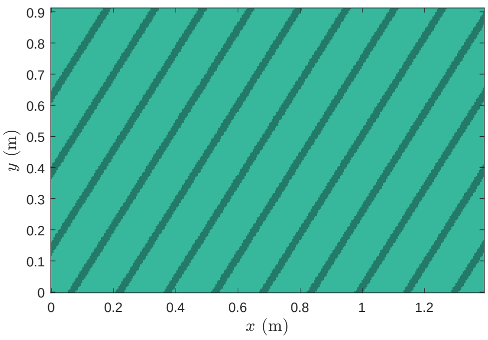

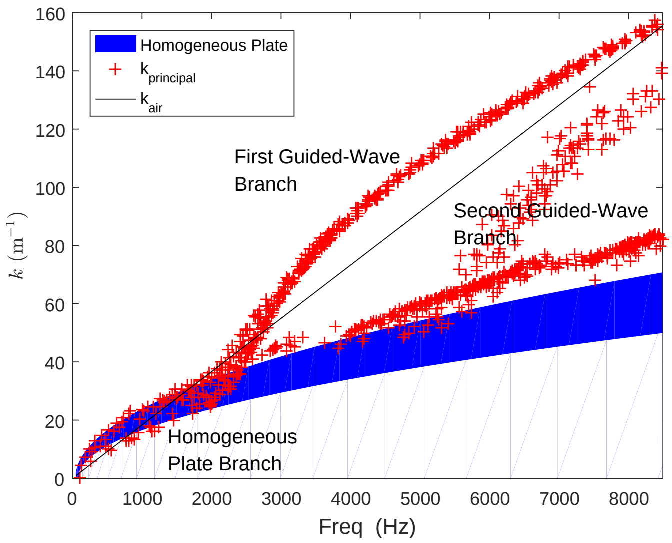

Figure 1: Left: The ribbed plate. Right: largest peak of all the modes as a function of the corresponding eigenfrequency (the oblique thin lines are a graphic artefact)

Since no dissipation is included in the mechanical model, the eigenvectors are real. These modal shapes are represented with real numbers (positive or negative) and no phase (no information is lost). Given that choice, a 2D Fourier transform has been applied to all modal shapes, yielding modal spectra $S_m(k_x, k_y) \in \mathbb{R}$.

As a first step, we extract the dominant peak $_{\text{principal}}$ from each spectrum. Its magnitude is represented in Fig. 1 as a function of the angular frequency of the corresponding normal mode. The figure displays three distinct branches which look like *dispersion branches*. However, one must keep in mind that data in this figure only represent a very partial view on the modes (limited to their principal wave-number).

Another view on all modes consists in adding all (spatial) spectral components in the (k_x, k_y)-plane. In such a representation, the eigenfrequencies are lost, as well as any form of visual clarity of the corresponding diagram (not represented). The interesting point is that clarity is retrieved when an appropriate ω-scaling is applied to the wave–number components k_x or k_y, as done in the next sections. The first scaling (Section 3) corresponds to a homogeneous-plate dynamics whereas guided-wave regimes (not completely understood at this point) correspond to the first and second branches (Section 4).

3 HOMOGENEOUS-PLATE BRANCH

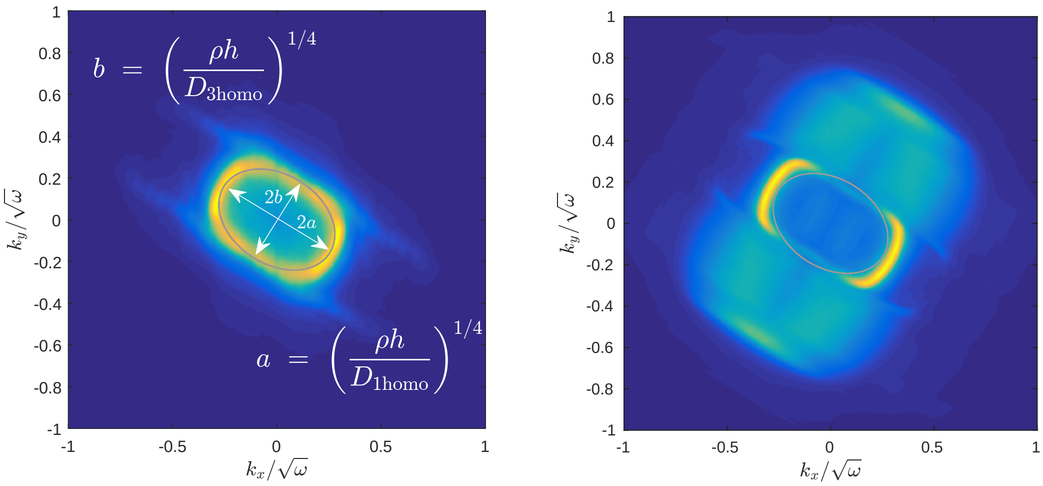

Figure 2: Dispersion maps. Left frame: scaling applied on modes with eigenfrequency below 2kHz. Right frame: same, on modes beyond 2kHz.

The dynamical equation ruling the transverse motion w of the non-homogeneous orthotropic thin plate is

$$\frac{\partial^2}{\partial X^2}\left(D_1\frac{\partial^2 w}{\partial X^2}\right)+\frac{\partial^2}{\partial X^2}\left(\frac{D_2}{2}\frac{\partial^2 w}{\partial Y^2}\right)+\frac{\partial^2}{\partial Y^2}\left(\frac{D_2}{2}\frac{\partial^2 w}{\partial X^2}\right)+\frac{\partial^2}{\partial Y^2}\left(D_3\frac{\partial^2 w}{\partial Y^2}\right)+\frac{\partial^2}{\partial X\partial Y}\left(D_4\frac{\partial^2 w}{\partial X\partial Y}\right)=\rho h(X,Y)\omega^2 w \tag{1}$$

where D_1 and D_3 on one hand, D_2 and D_4 on the other hand are of the form

$$D_{1,3}=\frac{E_{X,Y}h^3}{12(1-\nu_{XY}\nu_{YX})}\quad D_{2,4}=\frac{\nu_{YX}E_X h^3}{12(1-\nu_{XY}\nu_{YX})}+\frac{G_{XY}h^3}{6}\quad(\nu_{YX}E_X=\nu_{XY}E_Y) \tag{2}$$

The dynamical rigidities D are not constant over this non-homogeneous plate.

It is commonly accepted that homogenization theories can account for the dynamical behaviour of non-homogeneous plates at low frequencies only. Looking at Fig. 1, one can infer that more or less all modes below f_{H} (with $1.5 < f_{\text{H}} <$ 2kHz) could be described as normal modes of a homogeneous plate. Applying homogenization to the ribbed plate considered here, as in studies reported in [1], yields $E_{X\text{H}} = 1.45\times10^9$ Pa, $E_{Y\text{H}} = 5.51\times10^9$ Pa, $\rho = 227\,\text{kg}\,\text{m}^{-3}$ and $d_{\text{H}} = 16.9\,\text{mm}$ and the following dynamical equation for the equivalent homogeneous plate:

$$D_{1\text{H}}k_X^4+(D_{2\text{H}}+D_{4\text{H}})k_X^2k_Y^2+D_{3\text{H}}k_Y^4=\rho h_{\text{H}}\omega^2 \tag{3}$$

in the reciprocal space (k_X, k_Y). By construction, the homogeneous equivalent plate has an *elliptic* orthotropy: $D_{2\text{H}}+D_{4\text{H}}=\sqrt{D_{1\text{H}}D_{3\text{H}}}$.

With $K = k/\sqrt{\omega}$ (generic notation), Eq. (3) becomes

$$\frac{D_1}{\rho h}K_X^4+\frac{D_2+D_4}{\rho h}K_X^2K_Y^2+\frac{D_3}{\rho h}K_Y^4=1 \tag{4}$$

We represent the results of this rescaling on all the modal spectra in Fig. 2. By analogy with the "dispersion curve" terminology in the (ω, k)-plane, we call "dispersion map" this representation of the spectra of the normal modes.

Several features are quite remarkable here. (a) The left frame exhibits the expected homogeneous dynamical behaviour, but for *nearly all the spectral components* of the modes, not only the principal peaks. The figure is nearly elliptical and the expected quantities $D_{1\mathrm{H}}$ and $D_{3\mathrm{H}}$ are retrieved on the long and short axes respectively. (b) This homogeneous dynamics extends far beyond the upper frequency f_{H} beyond which the homogenization becomes invalid for describing the whole dynamics of the ribbed plate. This applies to *part of the spatial spectra*, as shown by the large blurry yellow zone, which does not follow this well-identified dynamics. (c) Above f_{H}, the elliptic homogenization is slightly altered.

4 GUIDED-WAVE BRANCHES

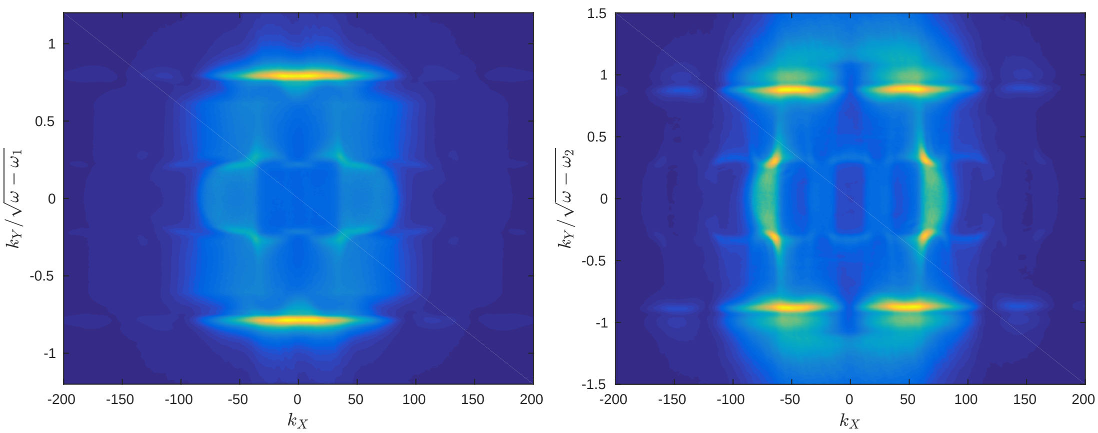

Figure 3: Dispersion maps with scaling by $\sqrt{\omega-\omega_{1,2}}$ applied to k_Y, the k_X-axis remaining unchanged. Each scaling is suited to one guided-wave branch. Left: all modes with an eigenfrequency above ω_1. Right: all modes with an eigenfrequency above ω_2.

We observe in Fig. 1 that above a transition occurring around $\approx 1.5 - 2$kHz, the principal wavenumber of the two additional branches is essentially driven by its k_Y-component. A more detailed analysis reveals that the k_X-components of the first guided-wave branch are all in the $[0, \pi/d]$ interval (more or less uniformly distributed) whereas the k_X-components of the second guided-wave branch are more scattered in the $[3\pi/(2d), 3\pi/d]$ interval: modes start to exhibit a guided-wave behaviour. As opposed to the previous section, the scaling here is by $\sqrt{\omega-\omega_{1,2}}$. Hypothetically, the cut-off frequency $\omega_{1,2}$corresponds, dynamically, to a low k_X, characteristic of the guided wave. An effective dynamical rigidity of the waveguide can be derived from Fig. 3. Surprisingly, its value appears to be less than that of the plate without ribs.

5 CONCLUDING REMARKS

Interestingly, the homogeneous and guided-wave regimes are not exclusive of each other. In fact, each mode tends to display some spectral components on each of the different branches (at least, above f_{H}).

REFERENCES

[1] Xavier Boutillon and Kerem Ege. Vibroacoustics of the piano soundboard: Reduced models, mobility synthesis, and acoustical radiation regime. *Journal of Sound and Vibration*, 332(18):4261–4279, 2013.